Biochimica et Biophysica Acta 1808 (2011) 26–33

Contents lists available at ScienceDirect

Biochimica et Biophysica Acta

journal homepage: www.elsevier.com/locate/bbamem

Effect of trehalose on the interaction of Alzheimer's Aβ-peptide and anionic lipid monolayers

Aslin Izmitli [a], Carolina Schebor [b], Michael P. McGovern [a], Allam S. Reddy [a], Nicholas L. Abbott [a], Juan J. de Pablo [a,*]

[a] Chemical and Biological Engineering, University of Wisconsin-Madison, 1415 Engineering Drive, Madison, WI 53706, USA
[b] Departmento de Industrias, Facultad de Ciencias Exactas y Naturales, Universidad de Buenos Aires, Ciudad Universitaria Ciudad Automa de Buenos Aires, Argentina

ARTICLE INFO

Article history:
Received 22 August 2009
Received in revised form 26 September 2010
Accepted 29 September 2010
Available online 1 October 2010

Keywords:
Amyloid beta peptide
Trehalose
Monolayer
Alzheimer's disease
Membrane

ABSTRACT

The interaction of amyloid β-peptide (Aβ) with cell membranes is believed to play a central role in the pathogenesis of Alzheimer's disease. In particular, recent experimental evidence indicates that bilayer and monolayer membranes accelerate the aggregation and amyloid fibril formation rate of Aβ. Understanding that interaction could help develop therapeutic strategies for treatment of the disease. Trehalose, a disaccharide of glucose, has been shown to be effective in preventing the aggregation of numerous proteins. It has also been shown to delay the onset of certain amyloid-related diseases in a mouse model. Using Langmuir monolayers and molecular simulations of the corresponding system, we study several thermodynamic and kinetic aspects of the insertion of Aβ peptide into DPPG monolayers in water and trehalose subphases. In the water subphase, the insertion of the Aβ peptide into the monolayer exhibits a lag time which decreases with increasing temperature of the subphase. In the presence of trehalose, the lag time is completely eliminated and peptide insertion is completed within a shorter time period compared to that observed in pure water. Molecular simulations show that more peptide is inserted into the monolayer in the water subphase, and that such insertion is deeper. The peptide at the monolayer interface orients itself parallel to the monolayer, while it inserts with an angle of 50° in the trehalose subphase. Simulations also show that trehalose reduces the conformational change that the peptide undergoes when it inserts into the monolayer. This observation helps explain the experimentally observed elimination of the lag time by trehalose and the temperature dependence of the lag time in the water subphase.

1. Introduction

Alzheimer's disease is associated with the formation of amyloid deposits generated by the polymerization of amyloidogenic Amyloid β-peptide (Aβ) [1,2]. Aβ peptide is an amphipathic molecule that is formed by proteolytical cleavage of the transmembrane amyloid precursor protein (APP) and is soluble in the plasma and cerebral vascular fluids [3,4]. The formation of fibrillar amyloid deposits is accompanied by conformational changes of the soluble peptide in the random coil or α-helical structure into β-sheet structures [5,6]. This is a nucleation dependent process where fibrillogenesis is facilitated by the formation of small amounts of aggregates. Lipid membranes have been studied as templates that facilitate the formation of the seeds for nucleation [7,8]. It has been shown that in the presence of lipid membranes, Aβ changes its configuration from a random coil to a beta-sheet or an alpha-helix [9–11] and the rate of aggregation is increased by three orders of magnitude [10,12]. The presence of additional components, such as gangliosides has been shown to accelerate the beta-sheet formation and aggregation processes [13].

Membrane model systems, such as monolayers, vesicles and supported bilayers have been utilized to study the effect of lipids on the structure of the peptide [14–18] and the effect of the peptide in the disruption of the lipid membranes [19–23]. In particular, Ege and Lee studied the insertion of Aβ into anionic (DPPG), cationic (DPTAP) and zwitterionic (DPPC) lipids and showed that insertion occurs mainly into anionic lipid membranes. They also performed dual-probe fluorescence measurements of the lipid and the peptide to study the surface morphology of the membranes and found that the peptide inserts into the expanded domains of the lipid membrane [24]. Kawasaki and coworkers studied the binding and adsorption of peptide aggregates on monolayers [25]. Grazing incidence X-ray diffraction and infrared reflection absorption spectroscopy measurements showed that Aβ absorbs into zwitterionic and anionic lipid monolayers in the uncompressed state adopting a β-sheet configuration [14,26]. More recently Chi and coworkers studied the effect of salts, pH and lipid charge on the

* Corresponding author. Tel.:+1 608 262 7727; fax: +1 608 262 5434.
E-mail addresses: cschebor@di.fcen.uba.ar (C. Schebor), abbott@engr.wisc.edu (N.L. Abbott), depablo@engr.wisc.edu (J.J. de Pablo).

0005-2736/$ – see front matter © 2010 Elsevier B.V. All rights reserved.
doi:10.1016/j.bbamem.2010.09.024

association of Aβ into lipid monolayers and the aggregation of Aβ in the presence of vesicles [27]. The effects of temperature and surface pressure on the kinetics of Aβ insertion into monolayers, however, do not appear to have been analyzed before. Kinetic information on Aβ insertion into lipidic interfaces could provide valuable insights into the process of fibril formation.

Several strategies have been considered to prevent or reduce Aβ aggregation. A variety of molecules have been considered as inhibitors of amyloid aggregation [28–33]. More recently, structural studies have been used to pursue the design of inhibitor molecules [34]. In particular, recent experiments indicate that, in bulk solutions, trehalose, a disaccharide of glucose, inhibits the aggregation of Aβ(1–40) and (1–42) [35,36]. Trehalose has also been proven to inhibit the aggregation of other amyloidogenic peptides in solution, including insulin [37] and polyglutamine peptides [38]. In the context of Huntington disease, trehalose has been shown to prevent the onset of the disease in a mouse model [38]. In a different context, trehalose is often used as an additive during lyophilization of proteins and cells, where it prevents damage to biological structures through a combination of direct and indirect interactions. Trehalose has been shown to interact with the phospholipid head groups of bilayer membranes [39] and has often been used as a cryoprotectant [40,41]. Recent molecular simulations of a *fragment* of Aβ, namely Aβ(29–40), in water and trehalose subphases have shown that in pure water the free energy of the peptide exhibits a broad minimum around disordered conformations, while in a trehalose subphase the α-helical conformation has a lower free energy [42]. Simulations have also shown that the peptide inserts into the DPPC bilayers in the α-helical configuration.

In this work, the effect of trehalose on the insertion of Aβ(1–40) into anionic DPPG monolayers at different temperatures and surface pressures is studied experimentally. Molecular simulations are also performed to analyze the effect of trehalose on the secondary structure of full Aβ and the free energy of the peptide during insertion into a monolayer. The mechanism of Aβ insertion into the monolayer and the role of trehalose on the dynamics of insertion are discussed.

2. Experimental methods

2.1. Materials

Synthetic β-Amyloid(1–40) was purchased from Anaspec (San Jose, CA). Stock solutions were prepared by dissolving the peptide in DMSO to reach a final concentration of 1 mg/ml. 1,2-Dipalmitoyl-sn-Glycero-3-[Phospho-rac-1-glycerol]sodium salt (DPPG) was purchased from Avanti Polar Lipids (Albaster, AL). Trehalose was purchased from Ferro Pfanstiehl Laboratories (Waukegan, IL).

2.2. Preparation of the monolayer

The surface pressure–area isotherms were obtained by means of a computer-controlled Langmuir Teflon-coated trough (KSV Minimicro System 1S, Helsinki, Finland) with a total surface area of 100 cm^2. The surface pressure was measured following a Wilhelmy-plate method using a roughened platinum plate connected to a microelectronic feedback system. Before starting the experiment, the trough was cleaned successively with ethanol and ultrapure deionized water. The trough was filled up with water and surface active impurities were removed by simultaneous sweeping and suction of the interface. The trough was thermostated using a water circulating bath. Monolayers were prepared by spreading the lipid solution on the aqueous subphase (pure water or 100 mM trehalose solution) using a Hamilton syringe. An equilibration time of 20 min was allowed before compressing the monolayer at 5 mm/min.

2.3. Constant pressure experiments

A constant surface pressure assay was used to monitor the insertion of the amyloid peptide in the DPPG monolayers. Experiments were performed by spreading DPPG onto a subphase free of peptide, and then compressing the lipid film to the predetermined surface pressure (25 mN/m or 30 mN/m). These pressure values were chosen to be close to the lipid-packing density of a bilayer [43] which is roughly equal to that of a monolayer at around 30 mN/m. Once the desired surface pressure was reached, it was kept constant. Fifty microliters of 1 mg/ml Aβ40 in DMSO was then aliquoted out, topped off with 0.2 ml water, and immediately injected into the subphase (50 ml) through an injection port using a syringe (Hamilton, Reno, NV). We have chosen to solubilize the peptide in DMSO because low concentrations of DMSO have been shown to have only a slight effect on phospholipid structure [44,45]. In contrast, recent experiments using HFIP, which is often used to solubilize Aβ, show that it accelerates the aggregation of amyloid peptides [46]. After peptide injection, the area was recorded along time. In this constant-pressure mode, insertion of the peptide into the lipid leads to an increase in the lipid surface area. The effect of temperature was examined in a range between 20 °C and 35 °C ± 1 °C using a water bath.

3. Computational methods

The simulated system, shown in Fig. 1, includes two monolayers of DPPG, with periodic boundary conditions, separated on one side by solvent and on the other side by vacuum. The initial structure of the Aβ(1–40) peptide was taken from a recent report obtained for implicit-membrane simulations [47]. That structure consists of two α-helical regions and two random coil regions. The monolayer membrane considered in this work included 64 DPPG molecules. The entire system was simulated using the Gromos96 53a6 force field, which has been shown to work well in lipid environments [48]. All simulations were performed at 300 K.

The initial structure of the monolayer was obtained by starting with an equilibrated DPPC bilayer generated in previous computational studies [39,49]. That structure was modified into a DPPG monolayer, and was then equilibrated for 10 ns, at which point the energy and structural characteristics were observed to converge. Initial structures for the system consisting of both the peptide and the monolayer were obtained by first running a series of expansions and energy minimizations of the membrane, then inserting the peptide, minimizing the energy, removing the peptide, contracting the system, and repeating the insertion until an appropriate lipid density was obtained, as described in by Kandt et al. [50]. As mentioned above, the full simulation box included two monolayers, one in the positive and one in the negative z-direction (normal to the monolayer) from the center of the box. The size of the simulation box was 5.14×5.14 nm in the x–y plane, while the total distance in the z-direction was approximately 8 nm, including the vacuum region.

Two different solvent systems were studied in this work: (a) pure water and (b) a 30%w/w trehalose/water mixture. Water molecules were modeled using the simple point charge (SPC) model [51]. For consistency, trehalose was also modeled using the Gromos 53a6 force field. Our simulations were performed with the Gromacs molecular simulation package [52]. Long-range electrostatic interactions were treated with a particle-mesh Ewald sum. The simulations were performed with rigid bonds (using the linear constraint solver method [53]) and with an integration time step of 2 fs. Multiple replicas of the system were set up with different distances in the z-direction between the center of mass of the peptide and the center of mass of the membrane. The range of distances varied such that at one extreme the peptide was 2 nm away from the center, on the solvent side, and at the other extreme it was 0.3 nm from the center, on the side closer to the vacuum region. Replicas were placed at regular

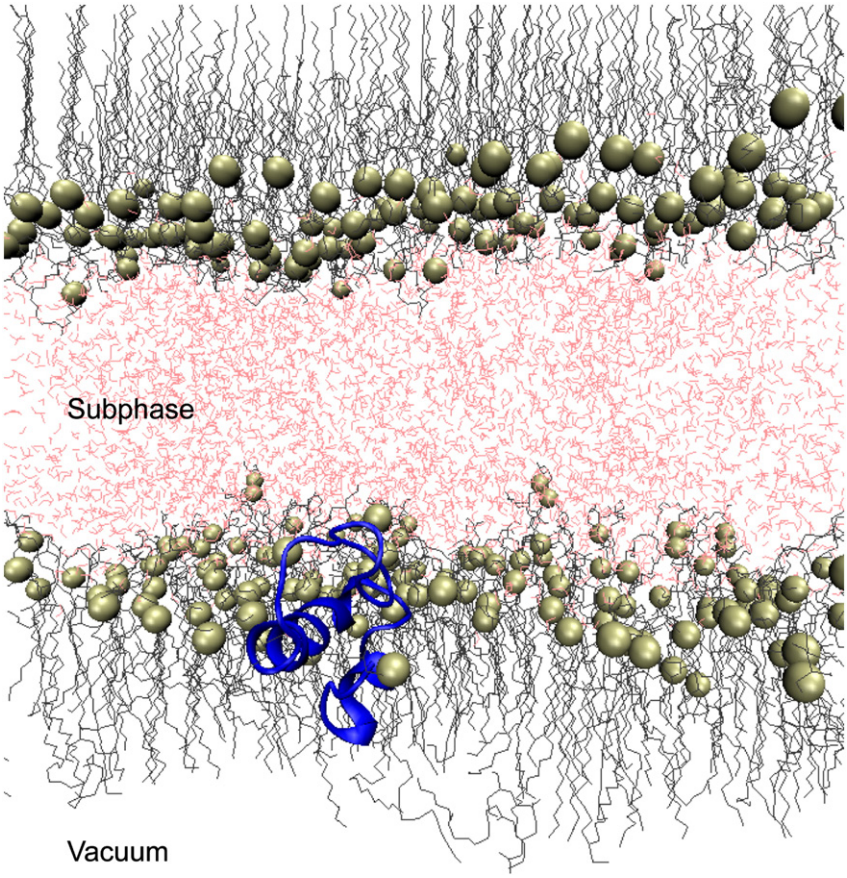

Fig. 1. Representative configuration of the simulation box. Along the *z*-axis, there are two monolayers of DPPG separated on one side by solvent and on the other side by vacuum. The *x* and *y* axes are periodic. The snapshot was rendered using visual molecular dynamics (VMD) [70].

intervals of 0.1 nm. The peptide–membrane *z*-distance was constrained in each replica and the force necessary to enforce this constraint was recorded. The system was simulated for 15 ns, and the first 4 ns of simulation time were excluded from the analysis to allow for equilibration. The mean force at each separation was determined and integrated to obtain a potential of mean force (PMF).

4. Results

Fig. 2 shows experimental data for the change in area as a function of time for a DPPG film spread on pure water at different temperatures. The DPPG monolayer was compressed up to 25 mN/m (Fig. 2a) and 30 mN/m (Fig. 2b), after which a constant-pressure experiment was performed. At these pressures, the monolayer is in the "liquid" or condensed branch of the pressure isotherms (see Fig. 3). The Aβ peptide was injected into the subphase and the area was recorded as a function of time to follow the peptide insertion. The constant-pressure curves exhibit a sigmoid shape consisting of a lag time and a growth phase. The increase in temperature causes a larger increase in the area. The area change is about three times larger for the monolayer compressed at 25 mN/m (Fig. 2a) than that at 30 mN/m (Fig. 2b). Also, at 30 mN/m, it is observed that the curves tend to reach saturation at lower areas than those compressed at 25 mN/m. This is consistent with the results of Terzi and coworkers [10], who reported that no insertion of peptide occurred at high surface pressures. In general, the results in Fig. 2 are consistent with those presented by Ege and Lee for the same system [24] and, as such, serve to validate our experimental methods and procedures.

It has been reported that the conformation of the Aβ in aqueous solution is predominantly random coil [54,55]. Experimental evidence suggests that, in order to insert into the monolayer, the peptide needs to adopt an α-helical structure [55–57]. Accordingly, upon injection of the peptide into the water subphase, the peptide would have to undergo a transition from a random coil to an α-helix prior to insertion into the monolayer. The time required for this transition could partly account for the observed lag time. Such conformational transitions are likely to be affected by temperature: it is observed that the lag time decreases with increasing temperature, but it is not altered to the same extent by the surface pressure of the monolayer (Fig. 2c). This last statement has been substantiated by constant-pressure experiments for 10 to 30 mN/m surface pressures at 30 °C (data not shown), which do not reveal a significant variation in the lag times. Given these results, it is proposed that, up to a pressure of 30 mN/m, the degree of compression of the monolayer is not a limiting step for peptide insertion.

To study the effect of trehalose on the interaction of Aβ with the DPPG monolayers, the insertion experiments were performed with a 100 mM trehalose subphase at 25 mN/m and 30 mN/m surface pressure and compared with the ones in a pure water subphase. Fig. 3a shows the compression isotherms for DPPG monolayers at 30 °C on water and 100 mM trehalose subphases. At a given pressure, the area density of the DPPG monolayer in the presence of trehalose is approximately 5 $Å^2$/molecule larger than in pure water. This observation is consistent with previous experimental observations [58]. Fig. 3b shows area versus time curves for DPPG films spread on a 100 mM trehalose solution at a surface pressure of 25 mN/m. The curves exhibit an exponential growth behavior, which differs considerably from the sigmoid shape observed in the pure water subphase (Fig. 2a). Furthermore, in the presence of trehalose, the kinetics of peptide insertion is not significantly affected by temperature. For all samples, the maximum area increase was reached 1 h after the peptide injection (Fig. 3b). In pure water (Fig. 2a), isotherms

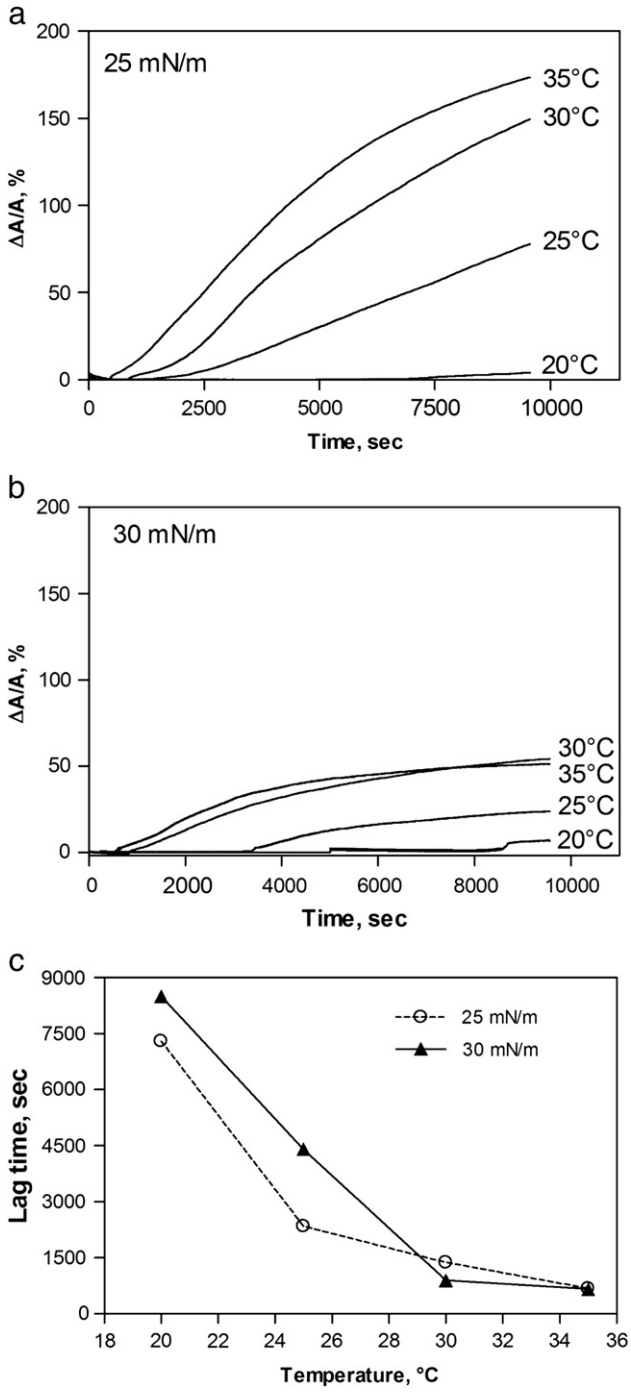

Fig. 2. Percent area change versus time curves of a DPPG film at constant surface pressure of (a) 25 mN/m and (b) 30 mN/m after injection of Aβ into the water subphase at time zero. (c) The lag time before insertion of Aβ into the DPPG monolayer begins versus temperature for 25 mN/m and 30 mN/m surface pressures of the monolayer.

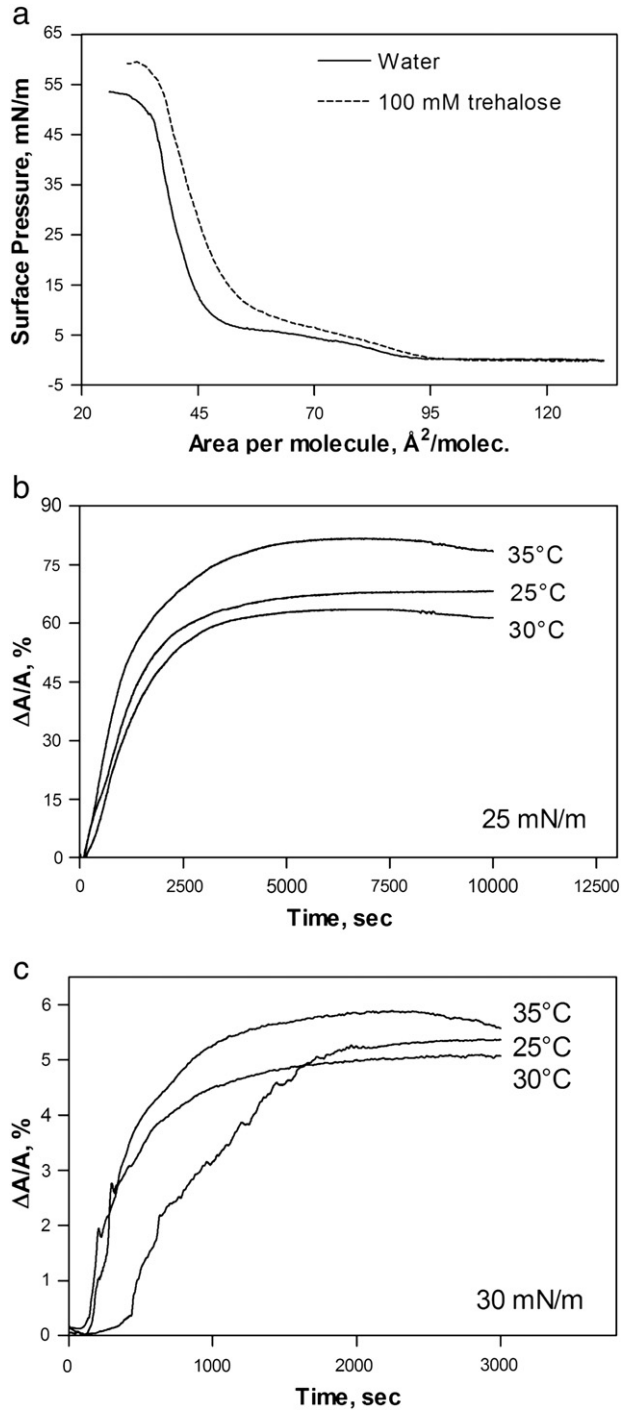

Fig. 3. (a) Compression isotherms of DPPG on water and 100 mM trehalose subphases. (b) Percent area change versus time curves of a DPPG film at constant surface pressure of 25 mN/m after injection of Aβ into 100 mM trehalose subphase at time zero. (c) Same as (b), but at a surface pressure of 30 mN/m.

collected at different temperatures exhibit pronounced differences; and none of the samples at 25 mN/m display a plateau during the time scale of our experiments. Fig. 3c shows the area increase versus time curves in 100 mM trehalose solution at 30 mN/m surface pressure. The extent of insertion is 10 times lower at this surface pressure and it is not affected by temperature. Note that, while the membranes are more expanded in the presence of trehalose, the actual terminal degree of expansion of the monolayer (the plateau region of Figs. 3b and c) is much smaller in trehalose than in pure water.

The compression isotherms of DPPG (Fig. 3a) show that at 25 mN/m surface pressure, the monolayer is 5 Å^2/molecule more expanded on the trehalose subphase. Fig. 4 shows the insertion of Aβ on the water subphase at 11 mN/m surface pressure, where the area per lipid molecule corresponds to the one at 25 mN/m on the trehalose subphase. The lag time before the peptide starts inserting into the monolayer is not affected by the expansion of the monolayer on the water subphase and the reduction of the surface pressure; only the rate and amount of insertion increase. This result shows that the vanishing of the lag time in 100 mM trehalose is not caused by the more expanded monolayer on this subphase.

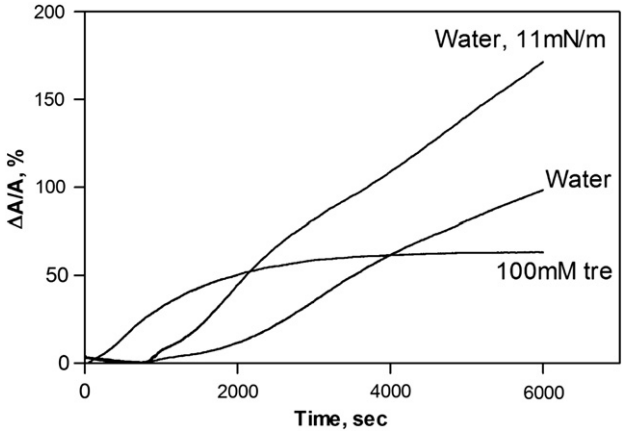

Fig. 4. Percent area change versus time curves at 30 °C on trehalose subphase at 25 mN/m and on water subphase at 11 mN/m and 25 mN/m. The area per lipid molecule at 11 mN/m on the water subphase corresponds to that at 25 mN/m on the trehalose subphase.

Fig. 5 shows results for the insertion of Aβ into a DPPG monolayer at different trehalose concentrations. The addition of trehalose does not have a significant effect at or below 10 mM concentration. The lag time is shorter at 50 mM and vanishes at 100 mM trehalose concentration.

In order to gain more insight into the observed differences in the insertion process, in particular the disappearance of the lag time and the decrease in the total amount of peptide insertion, we performed molecular simulations of the full Aβ(1–40) peptide and DPPG monolayer system. Fig. 6 shows the potential of mean force versus the constrained distance of the peptide and monolayer center of masses in water and trehalose subphases. The total peptide insertion in equilibrium is proportional to the integral of the Boltzmann factor of the free energy differences between the bulk and the monolayer surface. Consistent with our experimental observations, the curve for the water subphase exhibits a lower free energy minimum in the monolayer and it is wider, which both contribute to a larger integral and therefore a larger amount of peptide insertion at equilibrium. The minima of the PMF curves for the water and trehalose subphases are at 0.5 nm and 1 nm (center-of-mass COM distances) away from the monolayer. In pure water, Aβ(1–40) peptide inserts deeper into the monolayer (closer to the COM of the lipid monolayer) compared to the trehalose subphase, which could also contribute to a larger area increase for the water subphase.

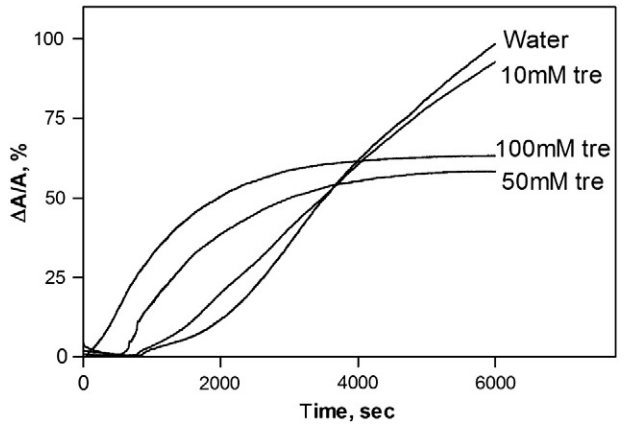

Fig. 5. Percent area change versus time curves of a DPPG film at constant surface pressure of 25 mN/m and 30 °C after injection of Aβ into 10 mM, 50 mM, 100 mM trehalose subphases and pure water at time zero.

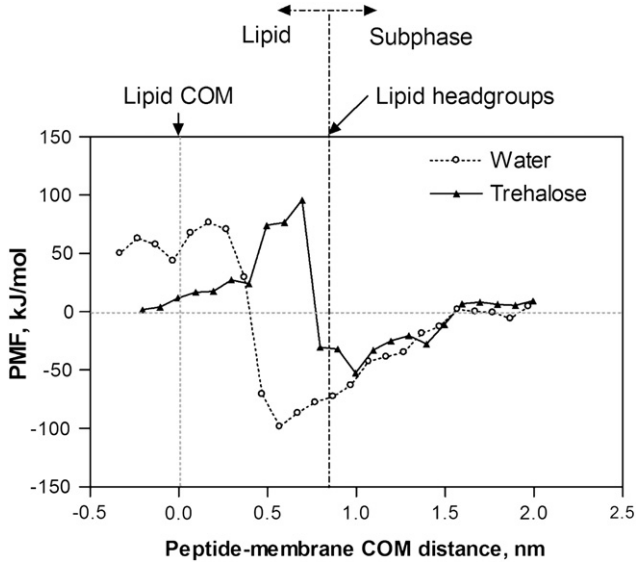

Fig. 6. Potential of mean force (PMF) versus the constrained center-of-mass (COM) distance of the peptide and the lipid monolayer for water and trehalose subphases.

Figs. 7(a) and (b) provide the percent helicity of Aβ(1–40) at each residue, in the water and trehalose subphases, respectively. The helicities are given in the bulk and in the monolayer. The monolayer positions are chosen to correspond to the free energy minima for

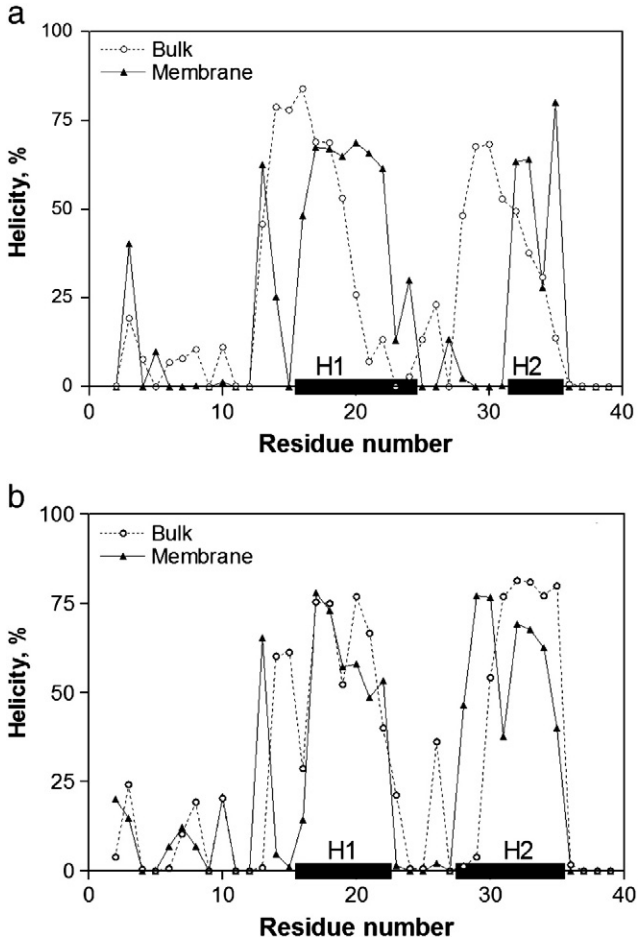

Fig. 7. Percent helicity for each residue of the Aβ(1–40) peptide in the bulk, and position of the free energy minimum for monolayer insertion in (a) water and (b) trehalose subphases.

insertion in each of the subphase conditions given in Fig. 6 (0.5 nm for water and 1 nm for trehalose subphases respectively). These figures show that in the bulk and in the monolayer, the peptide adopts a conformation that comprises a random coil and an alpha-helical region. Recent NMR studies of the human and rat islet amyloid polypeptide have shown that these peptides also fold into mixed random coil and alpha-helical domains in the presence of membranes [46,59–61].

A comparison of Figs. 7(a) and (b) shows that the peptide needs to undergo a larger conformational change in order to insert into the DPPG monolayer in the water subphase compared to the trehalose subphase. Quantitatively, the root mean square deviation (RMSD) of the percent helicities during monolayer insertion are 33% and 26% for the complete peptide in the water and trehalose subphases, respectively. In particular, for the hydrophobic end of the peptide, namely Aβ(29–40), which is believed to be largely responsible for insertion into cell membranes, the RMSDs of helicity changes are 36% and 20% for the water and trehalose subphases, respectively. These structural changes observed in simulations help explain why peptide insertion is easier in the trehalose subphase, and are consistent with the experimentally observed disappearance of the lag time with trehalose. Note that the overall helicity of the peptide in the bulk is 26% in water and 30% in trehalose. The increase in the helicity caused by trehalose is more dramatic in the hydrophobic end region of the peptide, Aβ(29–40), where trehalose increases the percent helicity from 25% (in water) to 44%.

It is of interest to analyze the orientation of the helical regions of the peptide when it is inserting into the monolayer. There are two undisturbed helical sections of the peptide for each subphase. These helical sections are marked on Figs. 7(a) and (b) as "H1" and "H2". Section H2 is located close to the hydrophobic C-terminus of the peptide, which is the end where the peptide starts inserting from. This result is consistent with previous NMR studies that showed that the amyloid β peptide exhibits two stable α-helical regions in the presence of negatively charged sodium dodecyl sulfate micelles [62,63]. Fig. 8(a) gives the angle between the helix axis and the plane of the monolayer for both of the helices in the water and trehalose subphases. The empty and filled symbols represent the first helix, H1, and second helix, H2, respectively. In the water subphase (circles), the angle is close to zero for both helices. This means that the helices orient themselves parallel to the surface of the lipid monolayer. In contrast, in the trehalose subphase (triangles), the hydrophobic C-terminus of the peptide adopts an average angle of 50° with respect to the monolayer. The positive sign of the angle indicates that the residue with the higher residue number, in this case M35, is closest to the monolayer. The second helix in trehalose makes an angle of about 20° to the monolayer surface and the negative sign indicates that the residue K16 is closest to the monolayer for this helix. The representative structures of the peptide at the monolayer surface are given in Figs. 8(b) and (c).

5. Discussion

We conducted the peptide insertion experiments at 25 mN/m and 30 mN/m surface pressures of DPPG. The lipid-packing density of a bilayer is roughly equal to that of a monolayer at around 30 mN/m

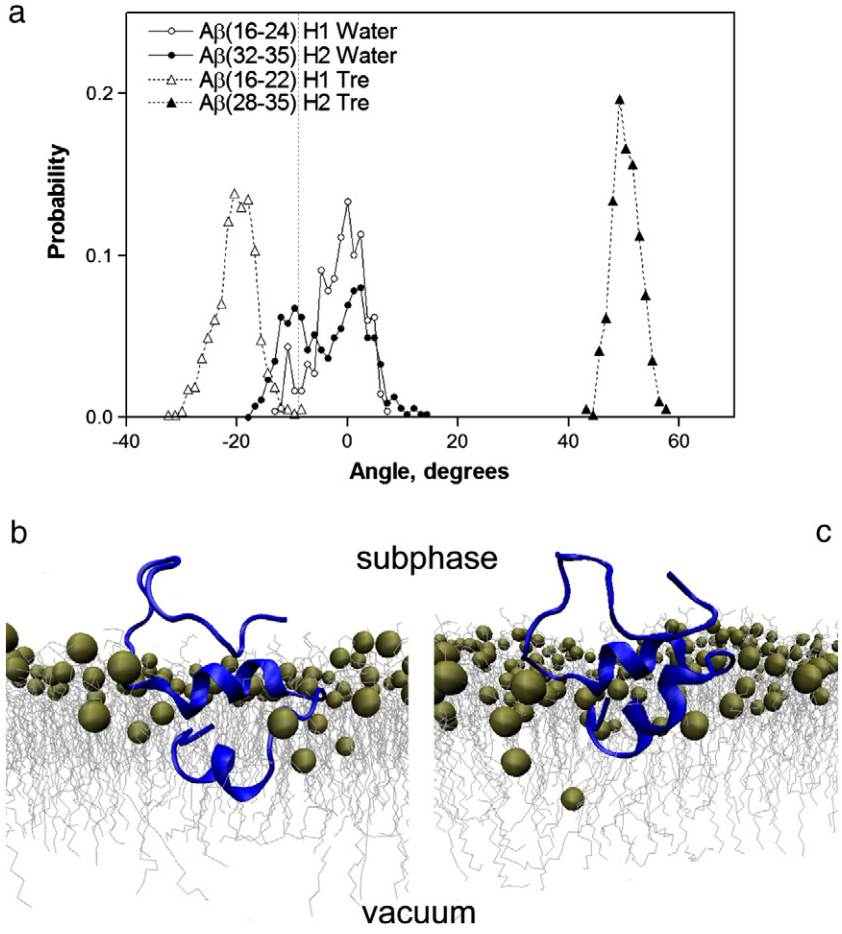

Fig. 8. (a) The angle between the helix axis and the plane of the monolayer for the two uninterrupted helical sections of Aβ(1–40) in water and trehalose subphases. (b,c) Representative configurations of the peptide inserted into the membrane in (b) water and (c) trehalose subphases. Snapshots were rendered using visual molecular dynamics (VMD) [70].

[43]. At this surface pressure the lipid monolayer is in the coexistence phase of the liquid expanded and condensed phases. Using fluorescently dyed lipid and peptide, the amyloid beta peptide has been shown to insert into the liquid expanded phase parts of the lipid monolayer [24]. We have chosen to do the experiments with purely negatively charged DPPG monolayers since amyloid beta peptide has been shown to interact more readily with negatively charged membranes [24]. The insertion of the peptide into the monolayer at these conditions is higher and therefore the effect of trehalose can be examined more easily.

On the water subphase, the constant-pressure curves exhibit a sigmoidal shape consisting of a lag time and a growth phase. An increase in temperature decreases the lag time, and increases the amount of insertion. There is a discontinuity in the insertion curves between 30 °C and 25 °C. This is because of a phase transition in the monolayer between these temperatures. The triple point of the DPPG monolayer on pure water is 23 °C [64]. Upon compression of the monolayer, the gas phase first transforms into the liquid expanded and then the liquid condensed phase above 23 °C, while it directly transforms into the liquid condensed phase below 23 °C. The insertion of the peptide into the monolayer is easier when the monolayer is in the liquid expanded phase. In pure water, increasing the surface pressure from 25 mN/m to 30 mN/m reduced the expansion of the monolayer by approximately a factor of three. Within the time scale of our experiments, the expansion of the monolayer in pure water does not reach a saturation, terminal value. In contrast, if the subphase includes 100 mM trehalose, the lag time vanishes and the peptide starts inserting immediately after injection into the subphase. Increasing the surface pressure from 25 mN/m to 30 mN/m causes a 10-fold decrease in the expansion of the monolayer. The monolayer becomes saturated after approximately 1 h, and the terminal degree of expansion is not particularly sensitive to temperature.

Results of simulations indicate that more peptide inserts in the water subphase, and that such insertion is deeper into the monolayer. Also, in the water subphase, the helical parts of the peptide at the C-terminus, which is the part that inserts into the monolayer, orients parallel to the monolayer. In contrast, in the trehalose subphase, the helical region at the hydrophobic C-terminus of the peptide makes an angle of 50° to the membrane, and occupies less space. These observations explain the larger area increase observed in experiments with a water subphase. Simulations also reveal that, in the water subphase, the secondary structure of the peptide undergoes considerable conformational changes, especially in the hydrophobic end region of the molecule. In contrast, such changes are relatively minor during insertion from the trehalose subphase. Such large conformational changes in the hydrophobic C-terminus of the peptide (or lack thereof in the trehalose subphase) help explain why the lag time for insertion is eliminated by the presence of trehalose. Since such changes would be faster at higher temperatures, this view of peptide insertion is also consistent with the experimental observation that the lag time (in water) decreases with increasing temperature.

Literature reports have argued that sugars are preferentially excluded from the vicinity of proteins in solution, leading to a preferential hydration of the proteins that favors a tight globular conformation [65–67]. We propose that trehalose causes the Amyloid β peptide to adopt a more α-helical conformation, especially in the hydrophobic end region, that is more readily inserted into the monolayer. Our current view is that, in aqueous solution, Aβ peptide needs to undergo a large change in its secondary structure in order to insert into the DPPG monolayer. In a trehalose solution, the peptide rapidly adopts a configuration which is similar to that in the monolayer, thereby reducing or eliminating the lag time for insertion. In the water subphase, the peptide can insert deeper into the monolayer and the free energy profile is broader, leading to larger peptide insertion and a correspondingly larger area increase.

Trehalose causes a dehydration of the lipid molecules; up to half of the hydrogen bonds between the lipid and water are replaced by trehalose molecules at concentrations above 20 mM [39,68]. Trehalose also decreases the dipole potential of the membrane. These effects may also be partially responsible for the disappearance of the lag time at high trehalose concentrations. The effect of trehalose on monolayers is believed to be comparable to that on bilayers [69]; the results of the Langmuir monolayer insertion experiments therefore provide insights into the effect of trehalose on the interaction of Aβ peptide with lipid vesicles as well.

We end our discussion with a few concluding remarks concerning the nature of the inserted peptide. In water, the monolayer expands considerably upon insertion. In trehalose, the extent of expansion is much more limited, and depends only slightly on temperature. However, at any given pressure, the monolayer is more expanded to begin with when trehalose is present. Based on that fact alone (a monolayer of lesser density), one would naively expect a greater degree of insertion and expansion in the presence of trehalose. To reconcile these seemingly contradictory observations, we speculate that insertion into the trehalose monolayer proceeds in a much more disorderly manner, with α-helical peptides rapidly inserting into the monolayer and reaching a dense, jammed state that is reminiscent of that encountered in amorphous solids, glasses, and colloids. In the water subphase, insertion proceeds much more gradually, thereby giving time for the monolayer to rearrange as more peptide is inserted and eventually absorb a greater amount of peptide, even if its density is higher.

Acknowledgments

J.J.d.P. and N.L.A. thank the NSF for support of this work through the University of Wisconsin Materials Research Science and Engineering Center on Nanostructured Interfaces. J.J.d.P. is also grateful to NSF for support through grant CBET-0755730.

References

[1] J. Hardy, Amyloid, the presenilins and Alzheimer's disease, Trends Neurosci. 20 (1997) 154–159.
[2] D.J. Selkoe, Normal and abnormal biology of the β-amyloid precursor protein, Annu. Rev. Neurosci. 17 (1994) 489–517.
[3] C. Haas, D.J. Selkoe, Alzheimer's disease: a technical KO of amyloid-bold beta peptide, Nature 391 (1998) 339–340.
[4] F.D. Cohen, J.W. Kelly, Therapeutic approaches to protein-misfolding diseases, Nature 426 (2003) 905–909.
[5] D.B. Teplow, Structural and kinetic features of amyloid beta-protein fibrillogenesis, Amyloid 5 (1998).
[6] D.M. Walsh, A. Lomakin, G.B. Benedek, M.M. Condron, D.B. Teplow, Amyloid beta-protein fibrillogenesis — detection of a protofibrillar intermediate, J. Biol. Chem. 272 (1997) 22364–22372.
[7] G.P. Gorbenko, P.K.J. Kinnunen, The role of lipid–protein interactions in amyloid-type protein fibril formation, Chem. Phys. Lipids 141 (2006) 72–82.
[8] J. McLaurin, D.S. Yang, C.M. Yip, P.E. Fraser, Review: modulating factors in amyloid-β fibril formation, J. Struct. Biol. 130 (2000) 259–270.
[9] E. Terzi, G. Hölzemann, J. Seelig, Self-association of β-amyloid peptide (1–40) in solution and binding to lipid membranes, J. Mol. Biol. 252 (1995) 633–642.
[10] E. Terzi, G. Hölzemann, J. Seelig, Interaction of Alzheimer β-amyloid peptide (1–40) with lipid membranes, Biochemistry 36 (1997) 14845–14852.
[11] V. Koppaka, P.H. Axelsen, Accelerated accumulation of amyloid β proteins on oxidatively damaged lipid membranes, Biochemistry 36 (2000) 10011–10016.
[12] J.A. McLaurin, A. Chakrabbartty, Characterization of the interactions of Alzheimer β-Amyloid peptides with phospholipid membranes, Eur. J. Biochem. 245 (1997) 355–363.
[13] K. Matsuzaki, K. Kato, K. Yanagisawa, A beta polymerization through interaction with membrane gangliosides, BBA Mol. Cell. Biol. L. 1801 (2010) 868–877.
[14] G. Brezesinski, E. Maltseva, H. Möhwald, Adsorption of amyloid β (1–40) peptide at liquid interfaces, J. Phys. Chem. 221 (2007) 95–111.
[15] S. Dante, T. Hauß, A. Brandt, N.A. Dencher, Externally administered amyloid β peptide 25–35 and perturbation of lipid bilayers, Biochemistry 42 (2003) 13667–13672.
[16] H. Lin, L. Bhatia, R. Lal, Amyloid β protein forms ion channels: implications for Alzheimer's disease pathology, FASEB J. 15 (2001) 2433–2444.
[17] M.J.O. Wildenbrandt, J. Rajadas, C. Sutardja, G.G. Fuller, Lipid-induced β-amyloid peptide assemblage fragmentation, Biophys. J. 91 (2006) 4071–4088.

[18] G. Thakur, M. Micic, R.M. Leblanc, Surface chemistry of Alzheimer's disease: a Langmuir monolayer approach, Colloid Surf. B 74 (2009) 436–456.
[19] C. Caughey, P.T. Lansbury, Protofibrils, pores, fibrils, and neurodegeneration: separating the responsible protein aggregates from the innocent bystanders, Annu. Rev. Neurosci. 26 (2003) 267–298.
[20] Y. Hirakura, B.L. Kegan, Channel formation in the pathogenesis of Alzheimer's disease and other amyloidoses, Einstein Q. J. Biol. Med. 16 (1999) 124–129.
[21] M. Kawahara, Y. Kuroda, Alzheimer's amyloid β-protein forms Ca2+-permeable channels in neuronal cells and its aggregation is stimulated by aluminum, J. Neurochem. 69 (1997) S46.
[22] H. Lin, Y.W.J. Zhu, R. Lal, Amyloid β protein (1–40) forms calcium-permeable, Zn2+-sensitive channel in reconstituted lipid vesicles, Biochemistry 38 (1999) 11189–11196.
[23] M.R.R. de Planque, V. Raussens, S.A. Contera, D.T.S. Rijkers, R.M.J. Liskamp, J.M. Ruysschaert, J.R. Ryan, F. Separovic, A. Watts, β-sheet structured β-amyloid(1–40) perturbs phosphatidylcholine model membranes, J. Mol. Biol. 368 (2007) 982–997.
[24] C. Ege, K.Y.C. Lee, Insertion of Alzheimer's Aβ40 peptide into lipid monolayers, Biophys. J. 87 (2004) 1732–1740.
[25] T. Kawasaki, K. Asaoka, H. Mihara, Y. Okhata, Nonfibrous β-structured aggregation of an Aβ model peptide (Ad-1α) on GM1/DPPC mixed monolayer surfaces, J. Colloid Interface Sci. 294 (2006) 295–303.
[26] E. Maltseva, A. Kerth, A. Blume, H. Möhwald, G. Brezesinski, Adsorption of amyloid β (1–40) peptide at phospholipid monolayers, Chembiochem 6 (2005) 1817–1824.
[27] E.Y. Chi, A. Winans, J. Majewski, G. Wu, K. Kjaer, K.Y.C. Lee, Lipid membrane templates the ordering and induces the fibrillogenesis of Alzheimer's disease amyloid-β peptide, Proteins 72 (2008) 1–24.
[28] O.Y. Bang, H.S. Hong, D.H. Kim, H. Kim, J.H. Boo, K. Huh, I. Mook-Jung, Neuroprotective effect of genistein against β amyloid-induced neurotoxicity, Neurobiol. Dis. 16 (2004) 21–28.
[29] L. Bergamaschini, E. Rossi, C. Storini, S. Pizzimenti, M. Distaso, C. Perego, A. De Luigi, C. Vergani, M.G. De Simoni, Peripheral treatment with enoxaparin, a low molecular weight heparin, reduces plaques and β-amyloid accumulation in a mouse model of Alzheimer's disease, J. Neurosci. 24 (2004) 4181–4186.
[30] J. Li, M. Zhu, A.B. Manning-Bog, D.A. Di Monte, A.L. Fink, Dopamine and L-dopa disaggregate amyloid fibrils: implications for Parkinson's and Alzheimer's disease, FASEB J. 18 (2004) 962–964.
[31] A. Nordberg, E. Hellstrom-Lindahl, M. Lee, M. Johnson, M. Mousavi, R. Hall, E. Perry, I. Bedgar, J. Court, Chronic nicotine treatment reduces β-amyloidosis in the brain of a mouse model of Alzheimer's disease (APPsw), J. Neurochem. 81 (2002) 655–658.
[32] K. Ono, K. Hasegawa, H. Nakiki, M. Yamada, Curcumin has potent anti-amyloidogenic effects for Alzheimer's β-amyloid fibrils in vitro, J. Neurosci. Res. 75 (2004) 742–750.
[33] M.B. Podlisny, D.M. Walsh, P. Amarante, B.L. Ostazewski, E.R. Stimson, J.E. Maggio, D.B. Teplow, D.J. Selkoe, Oligomerization of endogenous and synthetic amyloid β-protein at nanomolar levels in cell culture and stabilization of monomer by Congo red, Biochemistry 37 (1998) 3602–3611.
[34] S.S. Hindo, A.M. Mancino, J.J. Braymer, Y.H. Liu, S. Vivekanandan, A. Ramamoorthy, M.H. Lim, Small molecule modulator of copper-induced A beta aggregation, J. Am. Chem. Soc. 131 (2009) 16663–16665.
[35] R. Liu, H. Barkhordarian, S. Emadi, C.B. Park, M.R. Sierks, Trehalose differentially inhibits aggregation and neurotoxicity of β-amyloid 40 and 42, Neurobiol. Dis. 20 (2005) 74–81.
[36] Y. Miura, C. You, R. Ohnishi, Inhibition of Alzheimer amyloid β aggregation by polyvalent trehalose, Sci. Technol. Adv. Mat. 9 (2008) 24407–24412.
[37] A. Arora, C. Ha, C.B. Park, Inhibition of insulin amyloid formation by small stress molecules, FEBS Lett. 564 (2004) 121–125.
[38] M. Tanaka, Y. Machida, S. Niu, T. Ikeda, N.R. Jana, H. Doi, M. Kurosawa, M. Nekooki, N. Nukina, Trehalose alleviates polyglutamine-mediated gathology in a mouse model of Huntington disease, Nat. Med. 10 (2004) 148–154.
[39] M. Doxastakis, A.K. Sum, J.J. de Pablo, Modulating membrane properties: the effect of trehalose and cholesterol on a phospholipid bilayer, J. Phys. Chem. B 109 (2005) 24173–24181.
[40] S. Ohtake, C. Schebor, S.P. Palecek, J.J. de Pablo, Phase behavior of freeze-dried phospholipid–cholesterol mixtures stabilized with trehalose, BBA Biomembr. 1713 (2005) 57–64.
[41] J.V. Ricker, N.M. Tsvetkova, W.F. Wolkers, C. Leidy, F. Tablin, M. Longo, J.H. Crowe, Trehalose maintains phase separation in an air-dried binary lipid mixture, Biophys. J. 84 (2003) 3045–3051.
[42] A.S. Reddy, A. Izmitli, J.J. de Pablo, Effect of trehalose on amyloid β (29–40)-membrane interaction, J. Phys. Chem. 131 (2009) 085101/1-8.
[43] A. Blume, A comparative study of the phase transitions of phospholipid bilayers and monolayers, Biochim. Biophys. Acta 557 (1979) 32–44.
[44] Z.W. Yu, P.J. Quinn, Solvation effects of dimethyl sulphoxide on the structure of phospholipid bilayers, Biophys. J. 70 (1998) 35–39.
[45] A.K. Sum, J.J. de Pablo, Molecular simulation study on the influence of dimethylsulfoxide on the structure of phospholipid bilayers, Biophys. J. 85 (2003) 3636–3645.
[46] R.P.R. Nanga, J.R. Brender, J. Xu, G. Veglia, A. Ramamoorthy, Structures of rat and human islet amyloid polypeptide IAPP1–19 in micelles by NMR spectroscopy, Biochemistry 47 (2008) 12689–12697.
[47] N. Miyashita, J.E. Straub, D. Thirumalai, Structures of beta-amyloid peptide 1–40, 1–42, and 1–55 — the 672–726 fragment of APP — in a membrane environment with implications for interactions with gamma-secretase, J. Am. Chem. Soc. 131 (2009) 17843–17852.
[48] J.A. Lemkul, D.R. Revan, Perturbation of membranes by amyloid β peptide — a molecular dynamics study, FEBS J. 276 (2009) 3060–3075.
[49] A.K. Sum, R. Faller, J.J. de Pablo, Molecular simulation study of phospholipid bilayers and insights of the interactions with disaccharides, Biophys. J. 85 (2003) 2830–2844.
[50] C. Kandt, W.L. Ash, D.P. Tieleman, Setting up and running molecular dynamics simulations of membrane proteins, Methods 41 (2007) 475–488.
[51] H.J.C. Berendsen, J.P.M. Postma, W.F. van Gunsteren, J. Hermans, in: B. Pullman (Ed.), Intermolecular Forces, D. Reidel Publishing Company, Dordrecht, The Netherlands, 1981, pp. 331–342.
[52] D. van der Spoel, E. Lindahl, B. Hess, G. Groenhof, A.E. Mark, H.J.C. Berendsen, GROMACS: fast, flexible, and free, J. Comput. Chem. 26 (2005) 1701–1718.
[53] B. Hess, H. Bekker, H.J.C. Berendsen, J.G.E.M. Fraaije, LINCS: a linear constraint solver for molecular simulations, J. Comput. Chem. 18 (1997) 1463–1472.
[54] M. Bokvist, F. Lindstrom, G. Grobner, CD and NMR studies of aggregation of amyloid-β(1–40) peptide upon binding to model and raft membranes, Biophys. J. 84 (2003) 56A.
[55] S.-R. Ji, Y. Wu, S.-F. Sui, Cholesterol is an important factor affecting the membrane insertion of β-Amyloid peptide (Aβ1–40), which may potentially inhibit the fibril formation, J. Biol. Chem. 277 (2002) 6273–6279.
[56] M. Coles, W. Bicknell, A.A. Watson, D.P. Fairlie, D.J. Craik, Solution structure of amyloid β-peptide (1–40) in a water–micelle environment. Is the membrane-spanning domain where we think it is? Biochemistry 37 (1998) 11064–11077.
[57] C.C. Curtain, F.E. Ali, D.G. Smith, A.I. Bush, C.L. Masters, K.J. Barnham, Metal ions, pH, and cholesterol regulate the interactions of Alzheimer's disease amyloid-β peptide with membrane lipid, J. Biol. Chem. 278 (2003) 2977–2982.
[58] A. Izmitli, C. Schebor and J.J. de Pablo, Effect of trehalose on the interaction of human islet amyloid polypeptide with anionic lipid monolayers and membranes (submitted for publication).
[59] R. Soong, J.R. Brender, P.M. Macdonald, A. Ramamoorthy, Association of highly compact type II diabetes related islet amyloid polypeptide intermediate species at physiological temperature revealed by diffusion NMR spectroscopy, J. Am. Chem. Soc. 131 (2009) 7079–7085.
[60] A.S. Reddy, L. Wang, Y.S. Lin, Y. Ling, M. Chopra, M.T. Zanni, J.L. Skinner, J.J. de Pablo, Solution structures of rat amylin peptide: simulation, theory and experiment, Biophys. J. 98 (2010) 443–451.
[61] A.S. Reddy, L. Wang, S. Singh, Y.L. Ling, L. Buchanan, M.T. Zanni, J.L. Skinner, J.J. de Pablo, Stable and metastable states of human amylin in solution, Biophys. J. 99 (2010).
[62] K.J. Marcinowski, H. Shao, E.L. Clancy, M.G. Zagorski, Solution structure model of residues 1–28 of the amyloid beta peptide when bound to micelles, J. Am. Chem. Soc. 120 (1998) 11082–11091.
[63] H.Y. Shao, S.C. Jao, K. Ma, M.G. Zagorski, Solution structures of micelle bound amyloid beta (1–40) and beta (1–42) peptides of Alzheimers's disease, J. Mol. Biol. 285 (1999) 755–773.
[64] D.Y. Takamoto, M.M. Lipp, A. von Nahmen, K.Y.C. Lee, A.J. Waring, J.A. Zasadzinski, Interaction of lung surfactant proteins with anionic phospholipids, Biophys. J. 81 (2001) 153–169.
[65] T.Y. Lin, S.N. Timasheff, On the role of surface tension in the stabilization of globular proteins, Protein Sci. 5 (1996) 372–381.
[66] E.P. Melo, T.Q. Faria, L.O. Martins, A.M.G.c. Calves, J.M.S. Cabral, Cutinase unfolding and stabilization by trehalose and mannosylglycerate, Proteins 42 (2001) 542–552.
[67] G. Xie, S.N. Timasheff, The thermodynamic mechanism of protein stabilization, Biophys. Chem. 64 (1997) 25–43.
[68] M.D.C. Luzardo, F. Amalfa, A.M. Nuñez, S. Diaz, A.C.B. de Lopez, E.A. Disalvo, Effect of trehalose and sucrose on the hydration and dipole potential of lipid bilayers, Biophys. J. 78 (2000) 2452–2458.
[69] A. Skibinsky, R.M. Venable, R.W. Pastor, A molecular dynamics study of the response of lipid bilayers and monolayers on trehalose, Biophys. J. 89 (2005) 4111–4121.
[70] D. Frishman, P. Argos, Knowledge-based secondary structure assignment, Proteins 23 (1995) 566–579.